Development of optical fiber sensor probes for rapid remote *in-situ* spectroscopic measurements of biological samples.

H. Georg Schulze[a,c,d], L. Shane Greek[a,b], Michael W. Blades[c], Alan V. Bree[c], Boris B. Gorzalka[d], Karl-Friedrich Klein[e], and Robin F. B. Turner[a,b]

[a]Biotechnology Laboratory, The University of British Columbia, 237-6174 University Boulevard, Vancouver, B. C., Canada, V6T 1Z3

[b]Department of Electrical Engineering, The University of British Columbia, 434-2356 Main Mall, Vancouver, B. C., Canada, V6T 1Z4

[c]Department of Chemistry, The University of British Columbia, E257-2036 Main Mall, Vancouver, B. C., Canada, V6T 1Z1

[d]Department of Psychology, The University of British Columbia, 2136 West Mall, Vancouver, B. C., Canada, V6T 1Z4

[e]Fachhochschule Giessen-Friedberg, Wilh. Leuschnerstr.16, D-61169 Friedberg, Germany*

ABSTRACT

We have developed fiber-optic probes that facilitate rapid, simultaneous determination of multiple analytes, *in situ*, over a broad range of concentrations. Theoretical and empirical methods were used to design and characterize prototype probes that comprise a single small-diameter excitation fiber and multiple larger diameter collection fibers for the optimal collection of side- and back-scattered or emitted light, depending on the sample characteristics.

Prototypes were developed for use with pulsed ultra-violet resonance Raman spectroscopy, however, probes of this type are also suitable for use with other spectroscopic techniques such as fluorescence. Materials specifications, modelling methods, fabrication methods, and performance characteristics are described. Probes of our design are at present capable of measuring the aromatic amino acids in the 10 μM range and nM detection limits can be expected. We have also obtained ultraviolet Raman and resonance Raman spectra from proteins, DNA, amino acids, steroids, neurotransmitters, and alcohols with these probes

Key words: fiber optic probes, probe efficiencies, pulsed deep UV transmission, resonance Raman spectroscopy

1. INTRODUCTION

Analytes often have to be measured in their natural environment under hostile, remote, sensitive, or near-inaccessible conditions. Optical fibers provide a simple means for performing light emission measurements *in situ* and under difficult conditions. The aim of the interdisciplinary work undertaken and reported here was to develop a sensor with the following requirements: remote measurements; measuring a wide concentration range; real time measurements; concurrent multiple analyte detection; and measurements in complex aqueous media. To achieve these goals, we used ultraviolet resonance Raman spectroscopy to selectively enhance analyte signals in aqueous mixtures of multiple analytes, and optical fibers to rapidly perform these measurements remotely.

* Further author information -
H.G.S.: Email: schulze@unixg.ubc.ca
L.S.G.: Email: shaneg@ee.ubc.ca
M.W.B.: Email: blades@chem.ubc.ca; WWW: http://a103.chem.ubc.ca/uvrs.html
A.V.B.: Email: bree@chem.ubc.ca
B.B.G.: Email: bgorzalka@cortex.ubc.ca
K.-F. Klein: Karl-Friedrich.Klein@e2.fh-friedberg.de
R.F.B.T.(correspondence): Email: robint@ee.ubc.ca; Telephone: 604-822-6132; Fax: 604-822-2114

Remote fiber-optic linked Raman and resonance Raman spectroscopy allows the collection of Raman spectra on a large variety of solid, liquid, and gaseous samples with great ease. It requires no sample presentation in spinning cells or guided wires as typically used, no alignment with input/output optics, can be highly efficient, can reach otherwise inaccessible samples, and can be performed with small probes due to the small diameter of optical fibers.[1,2] However, in the past it has been impossible to perform pulsed ultraviolet resonance Raman spectroscopy with optical fibers due to the irreversible damage caused to the fiber by the intense ultraviolet radiation.

We are reporting here on how we have overcome this problem by developing a side-collecting probe with greatly enhanced sensitivity and by using a novel specialty fiber to transmit light to the sample.

2. OPTICAL FIBER CHARACTERIZATION

Optical fibers are cylindrical waveguides and have different light propagation abilities and mechanical attributes. Some fibers such as sapphire fibers have high laser damage thresholds but also high attenuation of deep UV wavelengths.[3] Silica fibers show good transmission in the deep UV (below 250 nm) depending on the cladding material used[4] and the OH^- content of the core.[5] In general, the different fiber characteristics depend on the core and cladding materials used, the dopants employed for refractive index adjustments, and the manufacturing processes used and so vary from manufacturer to manufacturer. For example, at 200 nm, fiber from one supplier has an attenuation of about 1 dB/m while fiber from a different supplier has an attenuation of about 2 dB/m. These values do not include attenuation effects due to the formation of reversible and irreversible color centers in the fiber.[6,7,8] This type of attenuation, however, can severely hamper pulsed UV transmission. Therefore, the optical fibers from different manufacturers had to be characterized with regard to their transmission and other physical qualities to enable the selection of the most suitable fibers for building an efficient pulsed UV resonance Raman probe.

2.1. Light transmission

Low UV attenuation fibers from 4 different suppliers, tested at 225-235 nm and ~0.20 mJ/pulse, produced strong

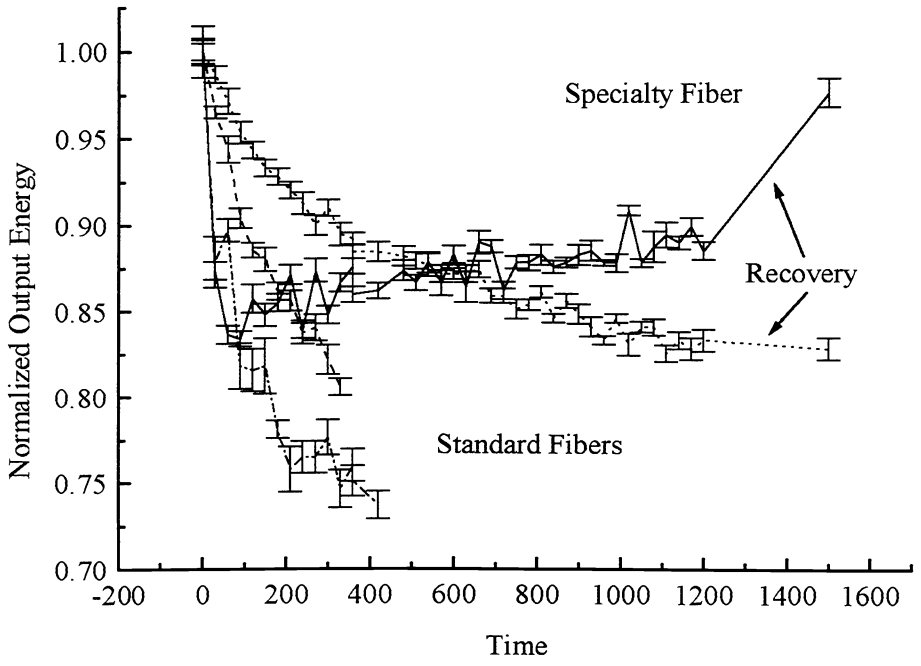

Figure 1. *The attenuation (mean ± S.E.M.; n = 10) for 15 cm sections of 300 μm fused silica fibers from 4 different suppliers, including a new experimental fiber for improved transmission of pulsed UV light (solid trace, top).*

attenuation which varied based on the manufacturer and on excitation wavelength. One of these was an experimental fiber aimed at providing improved UV transmission from pulsed light sources and a detailed characterization of the fiber is provided elsewhere.[9] Some of the throughput results for 15 cm sections of 300 μm fused silica fibers from different manufacturers are superimposed in Figure 1 for comparison. It can be seen from Figure 1 that the experimental fiber, despite its smaller 200 μm diameter, outperformed the other fibers both in terms of decay and recovery characteristics.

The efficiency of the same section of fiber was subsequently tested as a function of input energy. The input energy was incremented from about 80 μJ/pulse to about 250 μJ/pulse in 10 steps without any intervening recovery periods. The results indicated that the throughput efficiency of the fiber declined with increasing pulse energies. Output energies gradually increased and eventually exceeded 50 μJ/pulse. Although output energies in excess of 50 μJ/pulse could be achieved and sustained via a gradual increases in input energy, it could not be done with a single very large increment. Less large increments produced initial sharp declines in fiber throughput as shown in Figure 2 while small increments did not seem to produce these declines at all.

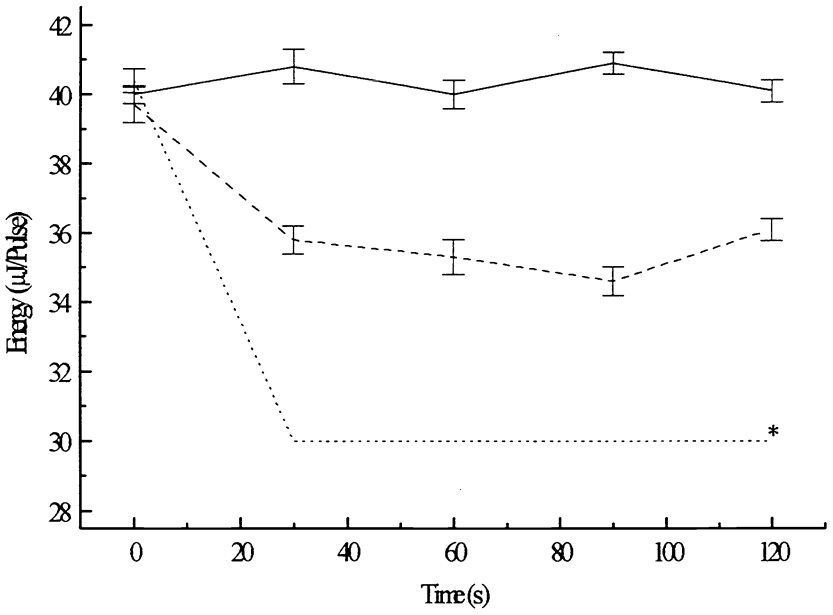

Figure 2. *The output energy as a function of time for fibers tested under 3 conditions: increasing the input energy with small increments (e.g. oscillator voltage from 640-646; solid line); with a moderate increment (590-615 V; dashed line), and with a large increment (590-639 V; dotted line) to the final operating level. Data were scaled to the same initial values. Asterisk indicates limit of instrument sensitivity.*

For example, when coupling about 203.43 ± 1.57 μJ/pulse (representing a 200 μJ/pulse increase) into a fresh 20 cm section of experimental fiber, the fiber output dropped to below the detection threshold after the first reading of 40.40 ± 0.35 μJ/pulse. When the experiment was terminated 5 minutes later, the output energy was still below the detection threshold. In contrast, an input of 217.50 ± 1.81 μJ/pulse (representing a 28 μJ/pulse increase), produced an output of 48.86 ± 0.16 μJ/pulse for at least 2 minutes when the previous input energy levels were attained via gradual increases. The moderately large pulse increase consisted of an input of 77.17 ± 1.15 μJ/pulse and produced a maximum decline of about 13%. These results indicated that a gradual step-wise increase in input energy was required to achieve high energy throughputs.

2.2. Beam profiles.

The spatial emission profiles from optical fibers of varying diameter were measured as part of the optical fiber characterization. Light from a HeNe laser (5 mW) was coupled into an optical fiber of given diameter and the emitted light was projected onto a Reticon 4096 element diode array detector (EG&G, Princeton, NJ). The fiber, 133 mm from the array, was mounted onto a translation stage that could be adjusted to move the beam incrementally across a mask containing a 1 mm slit covering the array. The readout from the array was moved to a microcomputer using Computerscope software via a Reticon 1020 interface and a ISC-16 data acquisition board. A C routine was used to convert the binary data to ASCII format. The results indicated that the emission beam profiles from smaller diameter fibers approached Gaussian distributions, but larger diameter fibers showed increasingly bimodal beam profiles. The central section beam profile of a 300 μm fiber is shown in Figure 3. Figure 3 reveals that although the beam profile of a 300 μm fiber can still be approximated by a Gaussian distribution, some bimodality is evident.

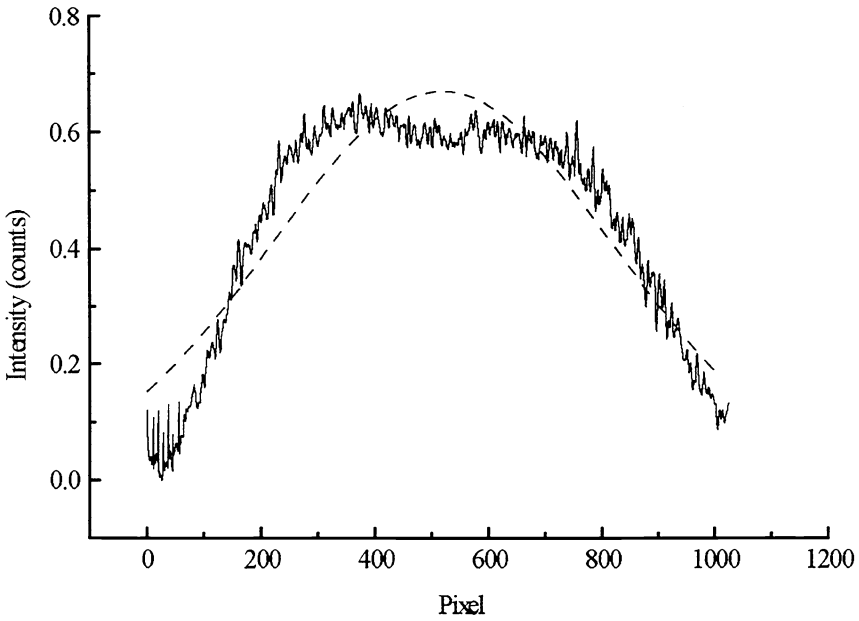

Figure 3. *The central section emission beam profile of a 300 mm fused silica fiber with a Gaussian fit (dashed line) superimposed for comparison.*

The temporal profile of the pulsed deep UV excitation beam was also measured. The light was obtained by pumping a Quanta Ray PDL-1 dye laser (Mountain View, CA) with the tripled (355 nm) output from a Lumonics HY-400 Nd:YAG laser (Rugby, U.K.) and frequency doubling the output with a CSK Optronics Super Doubler (Culver City, CA) using β-barium borate crystals to produce light in the 205-250 nm range. These measurements showed the pulsed deep UV light so obtained to have a significantly shorter pulse width (~3.3 ns, FWHM) than that of the original pump laser (11 ns, FWHM). These results are shown in Figure 4.

3. PROBE DESIGN

3.1. Design considerations

When using optical fibers for Raman spectroscopy, Raman and luminescence signals generated in the optical fiber core or cladding should be considered. Prominent Stokes shifted silica Raman features which can interfere with analyte signals occur at 1535, 817, and 516 cm^{-1} and are pronounced in long fibers,[10] while the anti-Stokes band near 500 cm^{-1} has also been observed.[11] In addition, strong Rayleigh scattering by the fiber may completely obscure the much weaker Raman signals generated by analytes.[12] Although the use of a single fiber for both excitation and collection is

efficient because of a complete overlap of excitation and collection volumes, the interference caused by Raman and Rayleigh scattering from the fiber itself favors a dual or multiple fiber arrangement.[13]

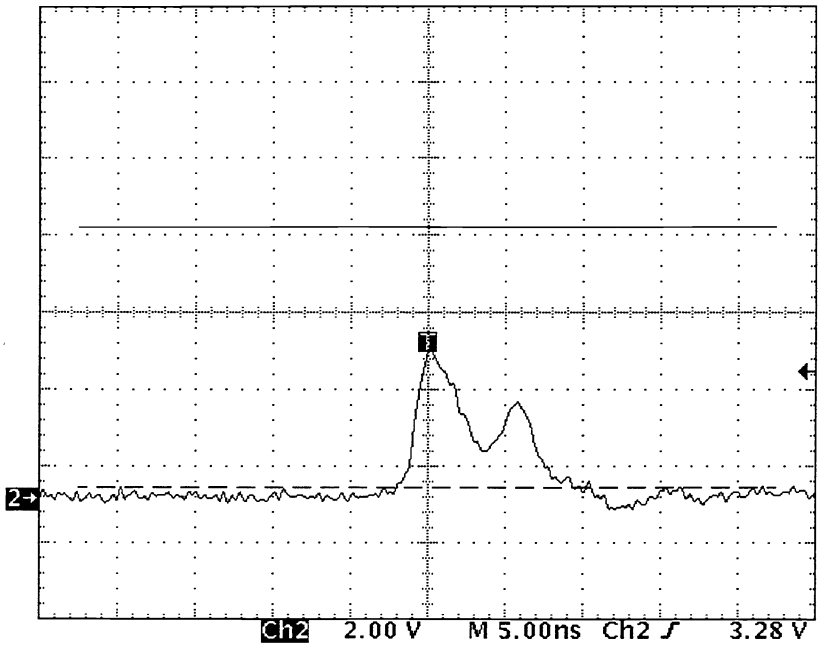

Figure 4. *The temporal beam profile of the pulsed deep UV light used in these experiments. Abscissa: 5 ns per division, ordinate: 2 volts per division.*

In a dual fiber geometry, one fiber is used for delivery of the excitation radiation, while another fiber is used to collect the scattered radiation from the sample. The fluorescence collection efficiency in a very dilute rhodamine 6G solution (~30 pM) was found to be optimal for small angles between collection and excitation fibers and poor for right angle collection.[14] The same advantage also benefits single excitation, multiple collection fiber arrangements. Such dual[12] and multiple fiber[1] probes have found applications in remote Raman spectroscopy. A forward scattering geometry is also efficient, but requires filters to remove the laser line[14] and Raman lines produced by the fiber[15] which could be impractical where very small probes are needed. For these reasons, it was decided to use separate excitation and collection fibers.

A knowledge of the excitation intensity profile was required in order to aid in the determination of the optimum probe geometry. A model was constructed to simulate (in Basic 4.0, Microsoft Corporation, Redmond, WA) different intensity profiles. Parameters that could be varied in the model included excitation and collection fiber diameters, separation distance between these fibers, numerical aperture, sample absorptivity, intensity gradations of the excitation light, and fiber tip geometry. A Gaussian beam profile with centered mean and 3 standard deviations across the fiber radius was often assumed for the exiting light, but could be changed if required. This assumption was justified by the results obtained from measuring the emission profiles from optical fibers as shown in Figure 3.

3.2. Fiber tip modifications

Due to internal filtering in samples with pronounced molar absorptivity, it is important for the excitation volume to be in close confinement to the collection fiber endface. This can be achieved by side-casting the excitation light across the collection surface. Figure 5 shows the simulated intensity distribution of light emerging from the excitation fibers of front- and side-casting probes, revealing a better overlap between excitation and collection volumes for the 90° geometry. Although the total analysis volume of the side-casting probe is smaller than that of the front-casting probe, Figure 5 reveals that those areas of the analysis volume of the side-casting probe excited by the most intense light fall within the acceptance cone of the collection fiber in contrast to the other arrangement where it falls mostly outside of the collection

cone. Figure 5 further reveals that the average distance from a volume element in the analysis volume of the side-casting probe to the collection face is shorter than the corresponding distance in the front-casting probe. Both considerations favor the side-casting probe in absorbing solutions and possibly in arrangements with restricted sample volumes. The positioning of the collection fiber endface relative to the excitation fiber tip (Figure 5, right-hand side), will affect the collection efficiency of the probe. Moving the endface of the collection fiber away causes more overlap between excitation and collection volumes. In particular, as the collection fiber endface is moved away from the excitation fiber tip, the efficiency of the probe should vary at different rates depending on the sample absorbance. We are presently modelling different probe geometries in order to determine their collection efficiencies in analytical samples of varying absorbance.

3.3. Excitation and collection fiber sizes

The effects of varying sizes of excitation and collection fibers were investigated with another model, the details of which have been reported elsewhere.[16] The results show that for a given diameter collection fiber, smaller excitation fibers are more effective. This is consistent with the fact that with smaller excitation fibers all the light energy gets "compressed" into a volume closer to the collection fiber which improves collection efficiency.

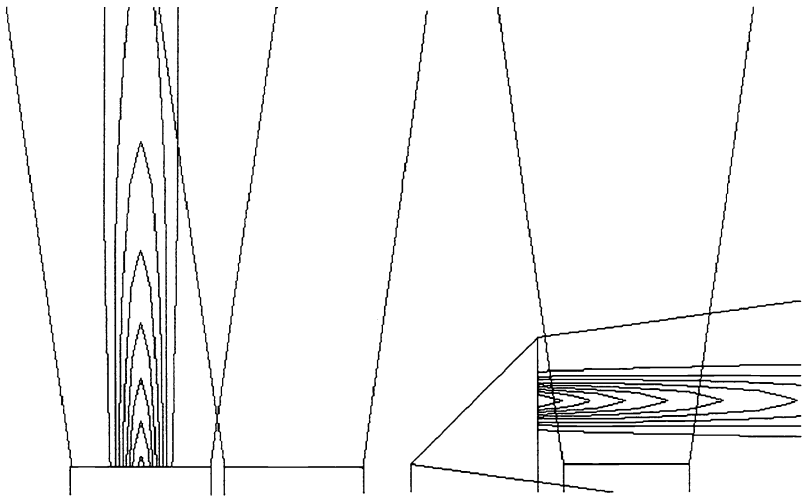

Figure 5. *The simulated intensity distribution of light emerging from the excitation fiber of a front-casting probe (left) and a side-casting probe (right).*

3.4. Bundles

For a given diameter excitation fiber, the collection efficiency of a probe can be increased by increasing the collection area of the probe. This can be accomplished by simply using a larger diameter collection fiber. An alternative method is to distribute the same area evenly around the excitation fiber by using several smaller diameter collection fibers. The alternative method has the benefit of distributing the collection area closer to the high intensity excitation, thus improving collection efficiency. Thus, using four 200 μm collection fibers should be four times better than one 200 μm collection fiber as well as better than using a single 400 μm collection fiber.

However, by using an angled excitation fiber, the collection area does not need to be distributed around the excitation fiber since all the excitation light can now be directed towards the collection fiber. Furthermore, if several excitation fibers are used and oriented to cast the excitation energy across a single central collection fiber, two advantages accrue: (i) more energy could be transmitted to the sample without risking damage to the probe and (ii) a high collection efficiency could be assured because the single collection fiber now substitutes for several collection fibers.

4. FIBER-OPTIC PROBE FABRICATION

4.1. End-face preparation

The quality of the fiber endfaces are crucial determinants of probe efficiency, especially if used for coupling high intensity excitation light into the fiber.[17, 18, 19] Good quality endfaces can be obtained by polishing or cleaving the fiber after stripping about 5 cm of jacketing material. Polishing was performed by hand using a Newport optical fiber chuck (FPH-DJ) to hold the fiber, gently applying pressure to the fiber tip while executing figures-of-eight on successively finer emery grit (600, 1200, and 4000) and lapping film (5 μm, 3 μm, 1 μm, and 0.3 μm). Cleaving was performed with a Newport fiber-optic cleaver (F-BK2) for 100 μm fibers and with a diamond scribe for larger fibers. The surfaces were then inspected under a microscope with 40x magnification for imperfections. If a bundle was to be assembled, the requisite number of fibers, plus a few additional ones in case of breakage, were cut to the desired length, the endfaces prepared, and more jacketing stripped if needed to yield about 5 cm of bare fiber.

If a UV reflective angled endface was needed, the chuck was held at the required angle while polishing. After polishing, about 1 cm of the angled tip was covered with positive photoresist (S1400-27) and baked in an oven at 95°C for 20 minutes to harden the photoresist. The fiber was removed from the oven and the angled facet lightly sanded with lapping film to remove the photoresist on the angled surface only. The surface was cleaned with deionized water to remove dust and grit. The angled tip was then inserted into a well in a vacuum chamber (CHA Industries Model SE-600-RAP, Menlo Park, CA) and positioned close to a vacuum deposition thickness gauge. The vacuum chamber was subsequently closed and aluminum deposited on the fiber by vacuum evaporation (~$2x10^{-6}$ Torr) to a thickness of 3/4 λ (for 250 nm the thickness was 187.5 nm) for optimum reflectance. After aluminum deposition, the fiber was removed and the tip inserted into warm acetone (~ 30°C) to remove the remaining photoresist from the protected areas of the fiber tip. An alternative method consisted of using aluminum pigmented acrylic paint and a very fine (#1) paintbrush to coat the endface. The latter method however, produced more diffuse than specular reflection.

4.2. Probe assembly

A collar made from a 0.5 mm section of 400 μm diameter silastic tubing was fitted around the end of one fiber by stretching it with a piece of wire (with ~300 μm diameter obtained from a stranded electrical wire) or a pair of small forceps. By repeating the process, a second fiber could be accommodated inside the same collar. When the wire was removed, the elastic tension in the silastic collar held the two fibers together about 1 mm from the probe tip. By gently rotating and pulling the longer fiber while holding the other fixed (e.g. with a piece of adhesive tape), the two fiber endfaces could be aligned with relative accuracy. The fibers were then permanently glued together.

Although multi-fiber probes with several excitation and several collection fibers could be made, it was easier to use either a single excitation fiber with multiple collection fibers or *vice versa*. The probe-end geometry of such probes always consisted of the single fiber (whether excitation or collection) in the center with the other fibers arranged around its perimeter. In order to obtain this geometry, the following procedure was followed. All the fibers were gently tied together, about 1 cm from their endfaces, with a section of thread. A silastic collar was then stretched in three directions with three separate pieces of wire making a triangular opening through which the bundle was fitted. Upon release the collar would hold all these fibers together. For example, the 8 angled excitation fibers (200 μm) and one flat end collection fiber (300 μm) shown in Figure 6 were fed through a silastic collar and held together during the assembly process.

At this stage, the fibers were not in their correct positions and considerable care and effort were required to gently nudge the central fiber with a sharp blade to the center of the bundle. An alternate method used consisted of inserting the central fiber through the collar first and then feeding the surrounding fibers one by one through the collar into position around it. The fibers were now aligned as described above. The individual surrounding fibers were labeled to facilitate the process. Where modified tips were used, fibers had to be aligned with respect to length as well as oriented with respect to angled surface. Light from a small HeNe laser was sequentially coupled into the one end of each surrounding fiber and the orientation adjusted until the deflected beam crossed the central fiber. When the alignment was satisfactory, the fibers were glued together. After the glue had completely cured, the probe tip was inserted into a glass pipette for protection. For measuring *in vitro* spectra, the probe was pushed forward until the tip protruded a little (~ 1 mm) from the pipette and for *in vivo* operation, the probe was removed entirely from the pipette.

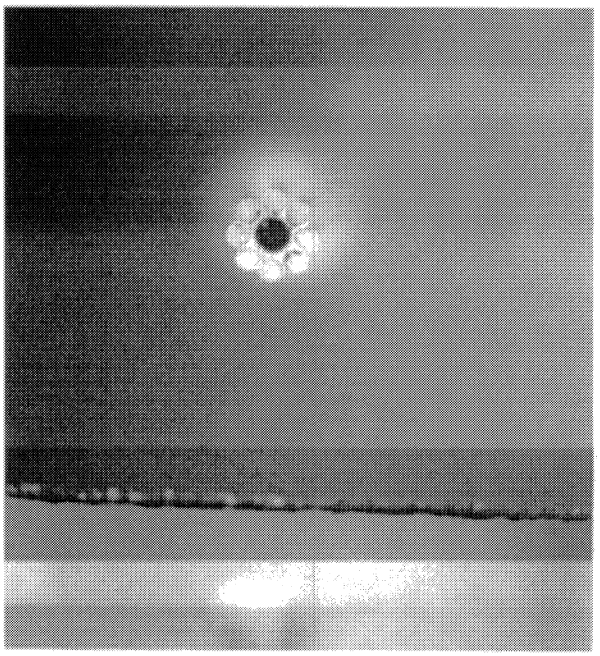

Figure 6. *End view of an optical fiber probe consisting of a central collection fiber (300 μm) surrounded by 8 angled excitation fibers (200 μm each).*

If the multiple fibers were to be used as collection fibers, no further assembly was required. For the purposes of coupling them to the spectrograph, a special chuck was machined in-house allowing the fibers to be lined up in front of the entrance slit. If multiple collection fibers were to be used as excitation fibers, their input ends had to be formed into a bundle. For this purpose, the fibers were packed as tightly as possible into a short section (~ 5 cm) of glass capillary tubing with internal diameter just large enough to accommodate them and with the bare fibers extending about 2 mm beyond the capillary. Often a suitable diameter tubing was not available and a larger diameter had to be used requiring one or more spacers.

4.3. Glue

Initially, an epoxy resin was used to glue the fibers together in the fabrication process. This proved unsatisfactory due to the large diameter probe tips that resulted from the very viscous resin. Furthermore, the biocompatibility of the substance was not known. It was therefore decided to use medical grade silicone rubber (Medical Adhesive Silicone Type A, Dow Corning, Midland, Michigan) which was certified biocompatible for implantations of less than 30 days. Silicone Type A could be mixed with cyclohexane to form an arbitrarily thin suspension. This gave a considerable degree of control over the thickness of the applied glue layer and hence over the final probe diameter. It was necessary, however, to increase the setting time of the glue suspension beyond the approximately 5 minutes available to allow for the correction of small alignment and orientation disturbances occurring during the gluing process. This was accomplished by adding tetradecane to the suspension (2:40:1 silicone rubber, cyclohexane, and tetradecane, respectively) to slow the vulcanization rate of the silicone rubber.

5. FIBER-OPTIC PROBE EVALUATION

5.1. Working curves

A mixture of a fixed concentration of 0.153 M KNO_3 and concentrations of methyl orange varying from 0-400 μM was used to determine the working curves for front-casting and side-casting probes. For each methyl orange concentration, 8 spectra of 5 s integration each, covering the range 1500 cm^{-1} to 1000 cm^{-1}, were collected with a specific probe *in situ*. The 473 nm line of an Ar^+ laser (Spectra Physics Stabilite 2017, Mountain View) was used for excitation and a single monochromator (McPherson Model 207, Acton, MA) for frequency decoding. The average height of the 1400 cm^{-1} methyl orange peaks and the 1050 cm^{-1} KNO_3 peaks from the 8 spectra were plotted against methyl orange concentration to establish the working curves.

5.2. Excitation fiber diameters

The working curves of two probes with the same collection fiber diameter (1000 μm) and varying excitation fiber diameters, 300 μm and 1000 μm, respectively, are shown in Figure 7. The optima of the two probes occurred at virtually the same methyl orange concentration. The increased separation distance between the fibers in the 1000 μm x 1000 μm probe should result in its reaching an optimum efficiency at a lower methyl orange concentration than the 300 μm x 1000 μm probe. However, the magnitude of the effect is hard to assess. On the other hand, the effect of a smaller excitation fiber is clear and in agreement with the qualitative predictions from the simulation: a smaller excitation fiber increases the probe's efficiency by exciting a smaller volume closer to the collection fiber, but more intensely, as discussed above.

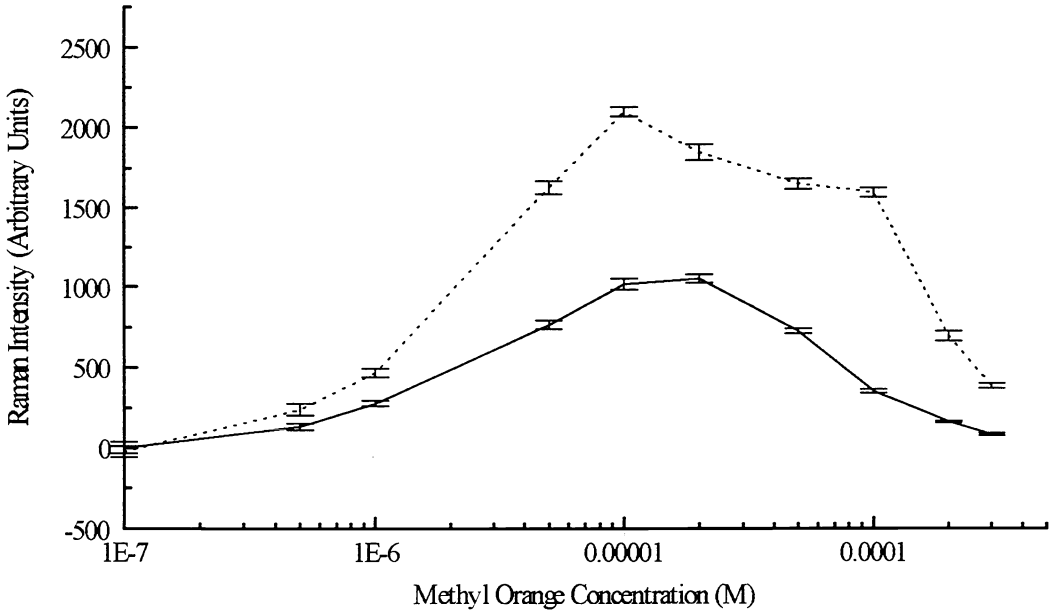

Figure 7. *The working curves of two front-casting probes with the same collection fiber diameter (1000 μm) and varying excitation fiber diameters, 300 μm (dotted line) and 1000 μm (solid line), respectively, normalized with respect to output power*

5.3. Fiber tip modifications

The effects of fiber tip modifications were investigated with a 200 μm x 200 μm front-casting probe and a 200 μm x 200 μm side-casting probe with aluminum pigmented acrylic paint or vacuum deposited aluminum applied to the angled facet of the excitation fiber to provide a reflective surface. The working curves for these three probes are shown in Figure 8. An inspection of Figure 8 shows that the side-casting probe reached its maximum efficiency at a higher methyl orange concentration than the front-casting probe. A better overall efficiency of the side-casting probe was predicted from the simulation. It is furthermore evident that the vacuum deposited reflecting aluminum surface gave the best efficiency.

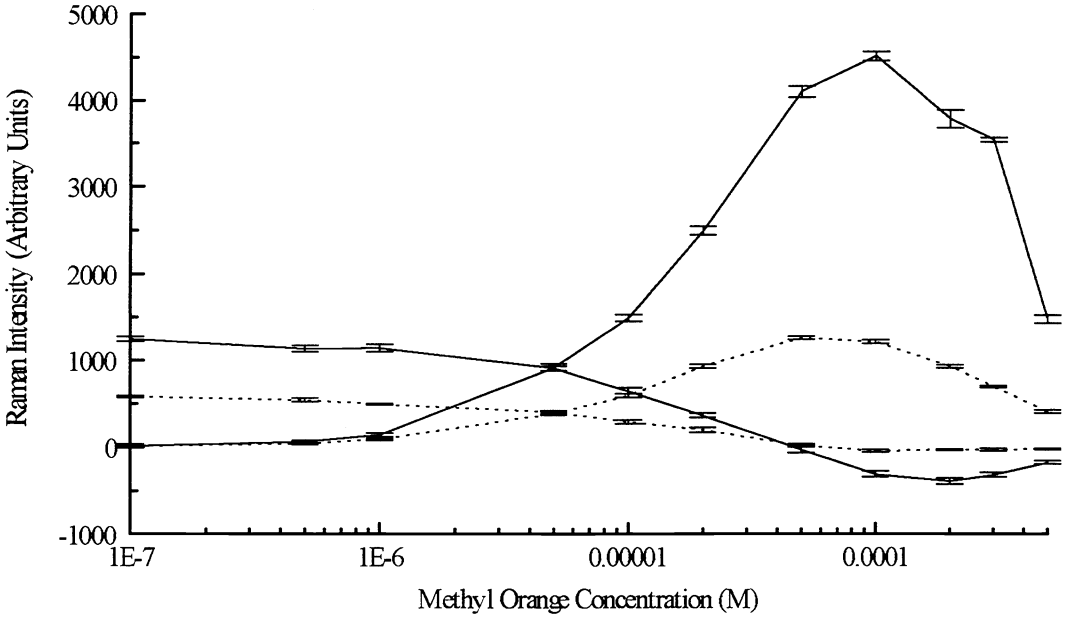

Figure 8. *The working curves of a 200* μm *x200* μm *front-casting probe (dotted line) and a 200* μm *x200* μm *side-casting probe (solid line) with aluminum pigmented acrylic paint. The working curves were normalized with respect to output power. KNO_3 peak intensities inversely related to methyl orange concentration, negative values are artifact. Methyl orange peak intensities reach maxima near 10^{-4} M.*

The suitability of the vacuum deposited aluminum coating for use in an excitation fiber was investigated by testing a 23.0 cm of 600 μm experimental fiber section with pulsed deep UV radiation, both with vacuum deposited Al mirrors at 45° to the fiber axis. The steady-state results are shown in Table I.

Table I

The input and output energies for a section of experimental improved UV transmission fiber (23.0 cm, 600 μm*) without modified tip, with angled tip and no reflecting material, and angled tip with reflecting material (vacuum deposited aluminum) at different deep UV wavelengths.*

Excitation λ (nm)	Input (μJ/pulse)	Output (μJ/pulse) Angled, no mirror	Output (μJ/pulse) Angled, mirror
230	48.9 ± 6.2	2.589 ± 0.019	4.138±0.029
230	76.3 ± 7.5	3.140 ± 0.016	8.605±0.054
230	102.9 ± 7.9	4.282 ± 0.020	9.972±0.051
		Non-angled	Angled, mirror
225	56.9 ± 7.7	18.41 ± 0.20	4.189±0.032

These results indicate that probes can be used in a configuration where the fiber with the angled facet is either used for excitation or collection. Moreover, they demonstrate improved transmission performance when a reflective coating is employed. However, the straight excitation with angled collection geometry appears to be the best.

5.4. Bundles

A probe with fiber-optic collection bundle was made and tested. This probe consisted of 1 central excitation fiber surrounded by 6 angled collection fibers. Contrary to the expected 6-fold improvement in performance of the probe compared to that shown in Figure 8, a high background which completely obscured the methyl orange signals was observed. Careful inspection of the probe under a microscope revealed that no air was trapped in the cavity formed by the collection fibers. It is therefore likely that the slight divergence of the excitation light cone produced multiple reflections inside the analysis cavity of this probe arrangement, necessitating the use of a laser line filter at the spectrometer entrance or a modification of the excitation fiber tip to focus the excitation light inside the analysis cavity. The latter modification would prevent excitation light from being directly reflected into the collection fibers.

6. CONCLUSIONS

The results from investigating different probe geometries experimentally and by simulation yielded important information for optimizing the design of fiber-optic probes for resonance Raman applications. From simulation and experiment the following requirements for constructing an efficient probe were established:

(i) small excitation fiber(s);
(ii) larger collection fiber(s);
(iii) confinement of the excitation volume close to the collection area; and
(iv) a collection area that can collect light from the entire excitation volume.

We have implemented these requirements by fabricating angled fiber-optic probes with vacuum deposited aluminum mirrors collecting at 90°. Several of these probes were used to successfully perform resonance Raman spectroscopy using pulsed deep UV excitation, therewith combining the convenience of optical fibers and the sensitivity of UV resonance Raman spectroscopy.

ACKNOWLEDGEMENTS

Financial support for this work was provided by Natural Siences and Engineering Research Council of Canada and the British Columbia Health Research Foundation. We have also received courteous and expert help from Dr. Alina Kulpa in the Department of Electrical Engineering and technical professionals in the mechanical, eletrical and glassblower's workshops of the Department of Chemistry. We are also indebted to Polymicro Technologies (Phoenix, AZ) for their kind supply of optical fiber samples.

REFERENCES

1. S. D. Schwab, and R. L. McCreery, "Versatile, efficient Raman sampling with fiber optics", Analytical Chemistry **56**, 2199-2204, 1984.
2. Z. Y. Zhu, and M. C. Yappert, "Determination of effective depth and equivalent pathlength for a single-fiber fluorometric sensor", Applied Spectroscopy **46**, 912-918, 1992.
3. R. S. F. Chang, Z. Ge, and N. Djeu, "UV-visible characteristics of sapphire fibers grown by laser-heated pedestal growth technique", *Proceedings of biomedical optoelectronic instrumentation*, J. A. Harrington, D. M. Harris, and A. Katzir (eds.), SPIE **2396**, 145-150, SPIE, Bellingham, 1995.
4. D. A. Krohn, and B. P. McCann, "Silica optical fibers: Technology update", *Proceedings of biomedical optoelectronic instrumentation*, J. A. Harrington, D. M. Harris, and A. Katzir (eds.), SPIE **2396**, 15-24, SPIE, Bellingham, 1995.
5. R. S Taylor, K. E. Leopold, R. K. Brimacombe, and S. Mihailov, "Dependence of the damage and transmission properties of fused silica fibers on the excimer laser wavelength", Applied Optics **27**, 3124-3133, 1988.
6. P. Karlitschek, K.-F. Klein, G. Hillrichs, and U. Grzesik, "Improved UV-fiber for 193 nm excimer laser applications", *Biomedical fiber optics*, A. Katzir and J. A. Harrington (eds.), SPIE **2677**, 127-134, SPIE, Bellingham, 1996.
7. K.-F. Klein, G. Hillrichs, P. Karlitschek, and U. Grzesik, "Improved optical fibers for excimer laser applications", LASERmed 95, paper 107b, in press, SPIE, Bellingham, 1995.
8. T. Toriya, K. Kaneda, T. Tsumanuma, and K. Sanada, "Characteristics of optical fiber for high power excimer laser", *Proceedings of biomedical optoelectronic instrumentation*, J. A. Harrington, D. M. Harris, A. Katzir (eds.), SPIE **2396**, 138-144, SPIE, Bellingham, 1995.
9. K.-F. Klein, L. S. Greek, H. G. Schulze, M. W. Blades, C. A. Haynes, and R. F. B. Turner, "Fiber-guided tunable UV-laserlight system around 215 nm", *Specialty fiber optics for biomedical and industrial applications*, A. Katzir, J. A. Harrington, (eds.), SPIE **2977**, in press, SPIE, Bellingham, 1997.
10. S. W. Kercel, M. J. Roberts, and A. A. Garrison, "Recent advances in the development of a fiber-optic based

instrument for on-line Raman analysis", *Raman and luminescence spectroscopies in technology II*, SPIE **1336**, 144-151, SPIE, Bellingham, 1990.
11. W. A. Gambling, and S. B. Poole, "Optical fibers for sensors", *Optical fiber sensors*, J. Dakin (ed.), 249-276, Artech House, Norwood, 1988.
12. D. Heiman, X. L. Zheng, S. Sprunt, B. B. Goldberg, and E. D. Isaacs, "Fiber-optics for spectroscopy", *Raman scattering, luminescence, and spectroscopic instrumentation in technology*, F. Adar, J. E. Griffiths, J. M. Lerner (eds.), SPIE **1055**, 96-104, SPIE, Bellingham, 1989.
13. M. L. Myrick, and S. M. Angel, "Elimination of background in fiber-optic Raman measurements", Applied Spectroscopy **44**, 565-570, 1990.
14. M. L. Myrick, S. M. Angel, and R. Desiderio, "Comparison of some fiber optic configurations for measurement of luminescence and Raman scattering", Applied Optics **29**, 1333-1344, 1990.
15. J. Ma, and Y. S. Li, "Optical-fiber Raman probe with low background interference by spatial optimization", Applied Spectroscopy **48**, 1529-1531, 1994.
16. L. S. Greek, H. G. Schulze, C. H. Haynes, M. W. Blades, and R. F. B. Turner, "Rational design of fiber-optic probes for visible and pulsed-ultra-violet resonance Raman spectroscopy", Applied Optics **35**, 4086-4095, 1996.
17. S. W. Allison, M. R. Cates, G. T. Gillies, and B. W. Noel, "Fiber optic pulsed laser delivery for remote measurements", Optical Engineering **26**, 538-546, 1987.
18. T. Beck, N. Reng, and K. Richter, "Fiber type and quality dictate beam delivery characteristics", Laser Focus World, October, 111-115, 1993.
19. T. De Hart, "Where and why optical fibers fail... and how to prevent it", Photonics Spectra, November, 107-110, 1992.